3-Chlorotyramine Acting as Ligand of the D$_2$ Dopamine Receptor. Molecular Modeling, Synthesis and D$_2$ Receptor Affinity

Emilio Angelina,[a, d] Sebastian Andujar,*[a, b] Laura Moreno,[c] Francisco Garibotto,[a, b] Javier Párraga,[c] Nelida Peruchena,[d] Nuria Cabedo,[e] Margarita Villecco,[f] Diego Cortes,[c] and Ricardo D. Enriz[a, b]

Abstract: We synthesized and tested 3-chlorotyramine as a ligand of the D$_2$ dopamine receptor. This compound displayed a similar affinity by this receptor to that previously reported for dopamine. In order to understand further the experimental results we performed a molecular modeling study of 3-chlorotyramine and structurally related compounds. By combining molecular dynamics simulations with semiempirical (PM6), ab initio and density functional theory calculations, a simple and generally applicable procedure to evaluate the binding energies of these ligands interacting with the D$_2$ dopamine receptors is reported here. These results provided a clear picture of the binding interactions of these compounds from both structural and energetic view points. A reduced model for the binding pocket was used. This approach allowed us to perform more accurate quantum mechanical calculations as well as to obtain a detailed electronic analysis using the Quantum Theory of Atoms in Molecules (QTAIM) technique. Molecular aspects of the binding interactions between ligands and the D$_2$ dopamine receptor are discussed in detail. A good correlation between the relative binding energies obtained from theoretical calculations and experimental IC50 values was obtained. These results allowed us to predict that 3-chlorotyramine possesses a significant affinity by the D$_2$-DR. Our theoretical predictions were experimentally corroborated when we synthesized and tested 3-chlorotyramine which displayed a similar affinity by the D$_2$-DR to that reported for DA.

Keywords: 3-Chlorotyramine · MD simulations · QTAIM analysis · D$_2$ dopamine receptor

1 Introduction

In the past the potential clinical usefulness of centrally acting dopamine receptor (DR) agonists has stimulated intense research on new dopaminergic agents. Thus, in general, different efforts in medicinal chemistry and neuropharmacology have yield substantial numbers of compounds with activity and selectivity at each of the major DRs.[1–6]

Particularly noteworthy is the work of Reutlinger, et al. who have recently reported the development and application of a computational molecular design method for obtaining bioactive compounds with desired on- and off target binding.[7] The authors used the molecular algorithm (MAntA)[8] which effectively transfers a nature-inspired optimization

[a] E. Angelina, S. Andujar, F. Garibotto, R. D. Enriz
Instituto Multidisciplinario de Investigaciones Biologicas (IMIBIO-SL -CONICET)
Chacabuco 915, 5700 San Luis, Argentina
phone: (54) 2652.423789
*e-mail: saanduja@unsl.edu.ar

[b] S. Andujar, F. Garibotto, R. D. Enriz
Facultad de Química, Bioquímica y Farmacia, Universidad Nacional de San Luis
Chacabuco 915, 5700 San Luis, Argentina

[c] L. Moreno, J. Párraga, D. Cortes
Departamento de Farmacología, Laboratorio de Fármacoquímica, Facultad de Farmacia, Universidad de Valencia
46100 Burjassot, Valencia, España

[d] E. Angelina, N. Peruchena
Laboratorio de Estructura Molecular y Propiedades, Área de Química Física, Departamento de Química, Facultad de Ciencias

Exactas y Naturales y Agrimensura, Universidad Nacional del Nordeste
Avda. Libertad 5460, (3400) Corrientes, Argentina

[e] N. Cabedo
Centro de Ecología Química Agrícola-Instituto Agroforestal Mediterráneo, Universidad Politécnica de Valencia, Campus de Vera
Edificio 6C, 46022 Valencia, España,

[f] M. Villecco
Instituto de Química Orgánica, Facultad de Bioquímica Química y Farmacia, Universidad Nacional de Tucumán
Ayacucho 471, S. M. de Tucumán, T4000INI. Argentina

🖥 Supporting Information for this article is available on the WWW under http://dx.doi.org/10.1002/minf.201400093.

principle to chemistry-driven molecular design; and they successfully designed antagonist compounds for the dopamine D4 receptor demonstrating the successful application of MAntA to dopamine receptors. However, despite the efforts of these authors, in general the design and development of DR-selective ligands remains largely empirical, quite conservative in following molecular precedents, somewhat unpredictable and not ready for routine applications of computer-aided drug design techniques. The computational limitations and/or errors can arise in many ways depending on the methodology: some possibilities include errors in the structure of the host, choice of ionization state, structure of the complex, inadequate sampling of internal degrees of freedom and the so called "ligand-receptor stereo-electronic problem."

In order to obtain new dopaminergic agonists, The dopamine molecule (compound **1** in Figure 1) has been modified on the amino group, on the ethylamine chain, and on the catechol moiety as well.[9–17] Claudi et al. reported the synthesis and binding affinity for D_1 and D_2 subtypes of DRs of 2-(4-fluoro-3-hydroxyphenyl)ethylamine (compound **7**, Figure 1).[16] This compound showed about two-fold lower affinity than dopamine for both binding sites. Previously Cardinelli et al reported low activity for other fluorine derivatives of dopamine including 2-(3-fluoro-4-hydroxyphenyl)ethylamine (compound **6**).[15] Studies on aminotetralins showed that 2-amino-6-chloro-7-hydroxytetralins (compound **8**) are weakly effective in the binding assays.[18] In

addition Claudi et al. reported that 2-chlorothyramine (compound **2**) is not able to discriminate between the two subtypes of dopamine receptors (D_1 and D_2), and has seven-fold lower affinity than dopamine for both sites.[17]

It must be pointed out that although 3-chlorotyramine (2-(3-chloro-4-hydroxyphenyl)ethanaminium chloride) (compound **3**) has been previously reported by Fuller[19] in 1971 and Stark and Fuller[20] in 1972; however, according to our bibliographic information, the dopaminergic effect of compound **3** has not been analyzed yet as a D_2-DR ligand. One possible explanation for this is that due to the low activity obtained for the analogues of this compound, compound **3** has been directly discarded as a potential ligand of interest for the D_2-DR.

The replacement of OH group by halogen introduces significant changes in the biological response of these ligands. For example it is interesting to note that in the series of benzazepines the 2,3,4,5-tetrahydro-7,8-dihydro-3-methyl-1-phenyl-1*H*-3-benzazepine (compound **9**) had only micromolar affinity at D_1 and D_2 receptors.[21] However 2,3,4,5-tetrahydro-7-chloro-8-hydroxy-3-methyl-1-phenyl-1*H*-3-benzazepine (compound **10**), obtained by replacing the 7-OH of **9** with a chlorine, has nanomolar affinity possessing a high selectivity by D1 receptors. In the same way our own studies performed on a series of benzyl-tetrahydroisoquinolines (BTHIQs) indicated that the presence of a chlorine group at C7 is very important for the adrenergic effect of such derivatives (compounds **11–14**).[22–24] In fact such BTHIQs possessing a chlorine group at C7 displayed the strongest affinity for both D_1 and D_2 DRs in this series.[23] It should be noted that the inductive effect of chlorine could influence the acidity of the phenolic group and produce different interactions at the binding pocket altering the affinity for D_2-DR. One question which arises is if compound **3**, which has not been previously studied as a D_2-DR ligand, have low or high affinity for this receptor and in either case try to find an explanation at sub-molecular level for such behavior. Another question which might arise is why to evaluate compound **3** and why now? There are different reasons to analyze this molecule with the computational approaches now available. On one hand it is possible to exploit recent information obtained for dopamine with respect to its biologically relevant conformation.[25] On the other hand is also now possible to study with some accuracy the electronic effects introduced to the ligand when replacing an OH by Cl and the effects of such change when the ligand is interacting with its biological receptor. Recently we reported a comprehensive conformational study of dopamine interacting with the D_2-DR, using a combination of molecular dynamics (MD) simulations, semiempirical and DFT calculations.[25] In addition, a detailed electronic analysis using Quantum Theory of Atoms in Molecules (QTAIM)[26–28] technique was also carried out. By using this approach it is possible to evaluate with some details the conformational and electronic behaviours of dopamine and its halogenated derivatives.
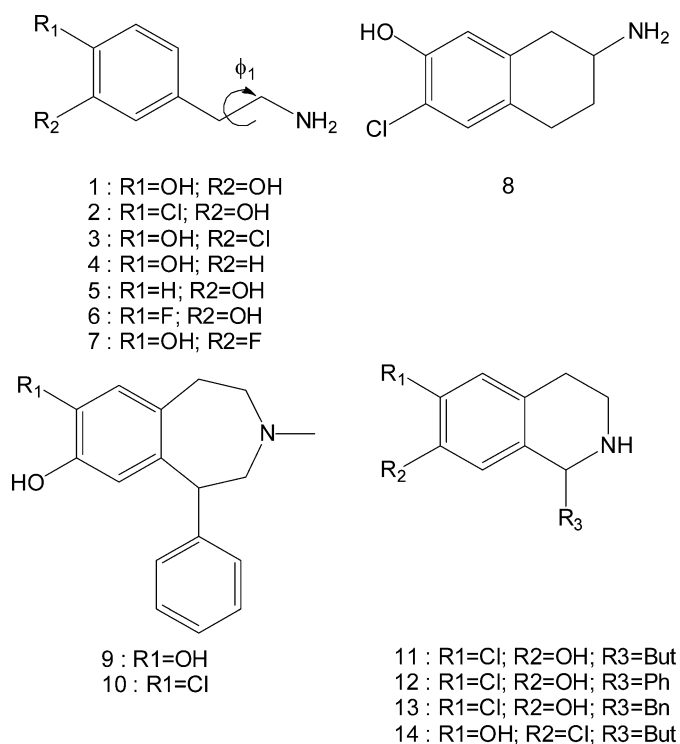

Figure 1. Structural feature of dopamine and derivatives.

1 : R1=OH; R2=OH
2 : R1=Cl; R2=OH
3 : R1=OH; R2=Cl
4 : R1=OH; R2=H
5 : R1=H; R2=OH
6 : R1=F; R2=OH
7 : R1=OH; R2=F

8

9 : R1=OH
10 : R1=Cl

11 : R1=Cl; R2=OH; R3=But
12 : R1=Cl; R2=OH; R3=Ph
13 : R1=Cl; R2=OH; R3=Bn
14 : R1=OH; R2=Cl; R3=But

Halogens, especially the lighter fluorine and chlorine, are widely used substituents in medicinal chemistry. Until recently, they were merely perceived as hydrophobic moieties and Lewis bases in accordance with their electronegativities. Much in contrast to this perception, compounds containing chlorine can also form directed close contacts of the type R—X·Y—R′, where the halogen X acts as a Lewis acid and Y can be any electron donor moiety. This interaction, referred to as "halogen bonding" since 1978[29] is driven by the σ-hole, a positively charged region on the hind side of X along the R—X bond axis that is caused by an anisotropy of electron density on the halogen.[30,31] The intriguing formal similarity between halogen bonding, R—X—B, and hydrogen bonding, R—H—B, has been noted and discussed in detail by Legon.[32,33] However, he also does point out that the hydrogen bond is more likely to be non-linear. In turn a halogen bond is a highly directional, electrostatically-driven non-covalent interaction between a region of positive electrostatic potential on the outer side of the halogen X in a molecule R—X and a negative site B, such as a lone pair of a Lewis base or the p-electrons of an unsaturated system. In a very elegant paper Politzer et al. have introduced the "σ-hole concept" allowing to explain the empirically-observed characteristics of halogen bonding: its marked directionality, its dependence upon the polarizability and electronegativity of the halogen atom, and the role of the electron-withdrawing power of the R portion of any molecule.[34]

In a recent review on different types of protein–ligand interactions relevant to medicinal chemistry,[35] the authors conclude that halogen bonds are a useful addition to the arsenal of favorable interactions in molecular recognition and can lead to significant affinity gains in some cases. There are a number of experimental studies where the effect of halogen substitution on binding affinity has been systematically evaluated.[36–38] The strengths of halogen bonds can be evaluated theoretically through quantum chemical model calculations. It is evident that halogen bonding is best described theoretically using high-level quantum chemical methods such as coupled cluster[39] (CCSD-(T)) and perturbation theory[40,41] (MP2) calculations; yet using these methods greatly limits the size of the model systems amenable to computational studies. Thus, much larger systems (like those studied here) can be treated using QM/MM calculations,[42,43] semiempirical studies[44] or using reduced model systems.[25]

Regarding the structural aspects of the D_2-DR it is well known that the binding of DA to the receptor is substantially affected by multiple serine/alanine mutations. The multiple mutations including a S193 susbstitution produce the greatest effect.[45,46] It has been previously reported that the effects of the multiple mutations were not additive, with the single serine mutation having relatively larger effects, which is indicative of a very precise network of hydrogen bonds between the TMV (transmembrane spanning region) serine residues and the catechol hydroxyls of the

DA molecule.[47] A further interesting finding was that addition of a 4-hydroxyl group (p-tyramine) to beta-phenylethylamine (compound **4**) does not enhance affinity, but addition of a 3-hydroxyl group (m-tyramine) (compound **5**) is favorable. When the 3-and 4- hydroxyls are present (the case of dopamine), the affinity is enhanced over the effects of the individual hydroxyl groups. These results are consistent with a productive and specific interaction of the two hydroxyl groups of DA with a network of serine residues. Our previous results[25] suggested that the region near these serine residues may be rather mobile which is consistent with a model of receptor function where the binding of DA locks the receptor into a relatively rigid conformation with precise interactions between ligand and receptor.

On the other hand it is well-known that the non covalent interactions generally are weaker than the covalent ones; such interactions are more difficult to describe properly. However, recent advances in computational calculation of the electron charge density make possible the proper description of the three-dimensional network of bonding and non bonding interactions in biological systems[27,48–50] in the context of the quantum theory of atoms in molecules (QTAIM).[51] Starting with strong and moderated hydrogen bonds or halogen bonds, moving on to weaker polar interactions and ending with stacking and T-shape interactions between aromatic rings, all of them can be evaluated by QTAIM analysis.[52] In fact, nowadays it is well know that the stacking amino acids aromatic rings in proteins is evidently much more important than it has been previously believed and, indeed, can form one of the dominant stabilizing contributions.[28] Our previous results show that the interactions of the catechol OH groups of the ligand, in the different conformations of the dopamine/D_2-DR complex, determine the decrease or increase of the electron density on the aromatic ring of dopamine. In turn, the electronic population of the aromatic ring of dopamine defines its orientation within the binding site and the type of interactions that are established with the aromatic rings of the receptor. It is evident that a description non quantum mechanical of the problem would overlook these electronic effects that are crucial to understand the binding modes of the ligand within the receptor binding site.

We were particularly intrigued to know which is the affinity of compound **3** by the D_2-DR and whether it was possible to explain such behavior through computational simulations. Thus, first we synthesized and tested compound **3** as a D_2-DR ligand. Whereas this compound showed an affinity comparable to that reported for dopamine in a second stage of our study we performed MD simulations for the complexes of compounds **1–5** with the D_2-DR. It should be noted that these compounds were carefully selected in function of their substituents at the catecholic portion. The selected compounds were: compounds **4** and **5** possessing only one hydroxyl group at *para* and *meta* position, respectively and compounds **2** and **3** possessing chlorine and hydroxyl groups at *para* and *meta* positions,

respectively. We also include in our comparative study dopamine (compound **1**), possessing the catecholic ring. The next step was to construct a reduced model for the binding site which allowed us to perform more accurate quantum mechanical calculations. The fourth step was to simulate the molecular interactions between the different ligands and the D_2-DR using a QTAIM analysis; being the principal goal of such calculations try to obtain a detailed description of the molecular interactions which stabilize and destabilize the different complexes. It is clear that a detailed analysis of the such interactions would be of paramount importance to determine the intricacies of the network of serine residues located at the binding pocket of the D_2-DR. Finally, we performed a comparative analysis among the different complexes and the conclusions are put forward in the last section.

2 Methods

2.1 Chromatographic and Spectroscopic Analysis

The reaction was monitored by analytical TLC with silicagel 60 F_{254} (Merck 5554). The residue was purified through silica gel C−18 (SPE, Alltech, 100 mg/1.5 mL) column chromatography. Isolation and purification was carried out by a Waters HPLC system with a 600 pump and both a 2996 Photodiode Array Detector (PDA) and ELSD 2420 Detector (Milford, MA). ^{1}H, NMR spectra was recorded on a Bruker AV 300 MHz instrument (Rheinstetten, Germany). Chemical shifts (δ) are reported in ppm for a solution of the compound in $CDCl_3$ and the coupling constants (J) values are given in Hz. High resolution ESIMS (electrospray) data were carried out on a Micromass Q-TOF Micro coupled with a HPLC Waters Alliance 2695 (Milford, MA). The instrument was calibrated by using a PEG mixture from 200 to 1000 MW (resolution specification 5000 FWHM, deviation < 5 ppm RMS in the presence of a known lock mass). The HCl salts of the synthesized compounds were prepared from the corresponding base with 5% HCl in MeOH. *N*-(4-benzyloxy)-3-chlorophenethyl)benzamide was prepared by standard methods from 3-chloro-4-methoxybenzaldehyde and benzoyl chloride.[22]

2.2 Synthesis of 3-Chlorothyramine (3)

A solution of the *N*-(4-benzyloxy)-3-chlorophenethyl)benzamide (1, 20 mg, 0.055 mmol) in a mixture of 2.5 N HCl/HOAc (4 : 1 mL) was heated for 42 h at 100 °C. Then, the solvent was removed under reduced pressure and the residue partitioned between H_2O/EtOAc. The phases were separated and the acid aqueous layer evaporated under reduced pressure to give a residue which was purified by column chromatography C−18 (SPE, Alltech, 100 mg/1.5 mL) and eluted in a gradient from 100% H_2O to 100% MeOH. The first fraction eluted with H_2O/MeOH (9 : 1) was evaporated and purified by semi-preparative HPLC using a Tracer Excel

120 ODS-B C18 column, 5 μm (25.0 × 1 cm), and MeOH/H_2O in 1% HOAc (20 : 80) as mobile phase with a flow of 2 mL/min. The 3-chloro-4-hydroxy-β-fenilethylamine (7 mg, 0.041 mmol, 75% yield) was isolated with a retention time (*Rt*) of 14.5 min as a white solid. ^{1}H NMR* (300 MHz, $CDCl_3$) δ 7.20 (s, 1H, H-2), 6.9 (s, 1H, H-6), 6.8 (s, 1H, H-5), 3.2 (m, 2H, CH_2-α), 2.8 (m, 2H, CH_2-β); ESMS *m/z* (%) 172 [M+1]$^+$ (39), 155 (100).

2.3 Binding Experiments

These experiments were performed on striatal membranes. Each striatum was homogenized in 2 mL ice-cold Tris-HCl buffer (50 mM, pH 7.4 at 22 °C) with a Polytron (4 s, maximal scale) and immediately diluted with Tris buffer. The homogenate was centrifuged on four times at 20000g for 10 min at 4 °C with resuspension in the same volume of Tris buffer between centrifugations. The final pellet was resuspended in Tris buffer containing 120 mM NaCl, 5 mM KCl, 1 mM CaCl2, 1 mM MgCl2 and 0.1% ascorbic acid (Tris-ions buffer), and the suspension was treated as described above. A 200 μL aliquot of freshly prepared membrane suspension (200 μg of striatal protein) was incubated for 1 h at 25 °C with 200 μL of Tris buffer containing [3H] raclopride (0.5 nM, final concentration) and 400 μL of Tris-ions buffer containing the drug under investigation. Non-specific binding was determined in the presence of 50 μM apomorphine and represented around 5–7% of the total binding. In both cases, incubations were stopped by addition of 3 mL of ice-cold buffer (Tris-Mg buffer or Tris-ions buffer, as appropriate) followed by rapid filtration through Whatman GF/B filters. Tubes were rinsed with 3 mL of ice-cold buffer, and filters were washed with 3×3 mL ice-cold buffer. After the filters had been dried, radioactivity was counted in 4 mL BCS scintillation liquid at an efficiency of 45%. Filter blanks corresponded to approximately 0.5% of total binding and were not modified by drugs.

2.4 Molecular Modeling

A 3D model of the human D_2-DR was used for the MD simulations. This model is based on the homology model from the crystallized D_3-DR, β_2 adrenoreceptor and A2α adenosine receptor as templates.[49,53,54]

Molecular docking simulations were performed with AutoDock4 program[55] using rotatable bonds in the ligands and flexible side chains in selected amino acids of the fifth transmembrane domain due to its implication in the formation of binding pocket.[47] Assignation of atomic partial charges (Gasteiger), rotable bonds as well as merging of non-polar hydrogens were performed with AutoDock Tools 1.5.2.[55] The ligands were then docked inside a cubic GRID box (70×70×70 Å, grid points separated by 0.375 Å) centered at the midpoint between the D114 and S194 alfa carbons (both residues conserved at the D_2-DR putative binding site). This docking simulation was achieved under the

hybrid Lamarckian genetic algorithm with an initial population of 100 randomly placed individuals and a maximum number of energy evaluations set at 1×10^7. All of the other parameters were maintained at their default settings.[55] The resulting docked orientations within a root mean square deviation (*RMSD*) of 0.5 Å were clustered together. From the lowest energy cluster, the best ranked conformation for each compound was then soaked in boxes of explicit water using the TIP3P model[56] and subjected to MD simulation. All MD simulations were performed with the Amber software package (All-atoms force field FF99SB)[57,58] using periodic boundary conditions and cubic simulation cells. The particle mesh Ewald method (PME)[59,60] was applied using a grid spacing of 1.2 Å , a spline interpolation order of 4 and a real space direct sum cutoff of 10 Å. The SHAKE algorithm was applied allowing for an integration time step of 2 fs. MD simulations were carried out at 300 K target temperature and extended to 10 ns overall simulation time. Positional restraints were applied to all the backbone alpha carbons of the receptor except those of the transmembrane 5 (TM5) domain that were left free. The NPT ensemble was employed using Berendsen coupling to a baro/thermostat (target pressure 1 atm, relaxation time 0.1 ps). Post MD analysis was carried out with program PTRAJ.[57]

2.5 MM-GBSA Free Energy and Per-Reside Decomposition Analysis

The MM-GBSA protocol was applied to calculate the relative binding energies of the complexes by taking snapshots at 10 ps time intervals from the last 1000 ps of the MD trajectory.

In order to determine the residues involved in the complexes intermolecular interactions, a per-reside free energy decomposition analysis using the mm_pbsa program in AMBER[61,62] was performed.

2.6 Quantum Mechanics Calculations and Topological Study of the Electron Charge Density Distribution

Reduced 3D models systems representing the D_2-DR binding pocket in the five molecular complexes **1**/D_2-DR, **2**/D_2-DR, **3**/D_2-DR, **4**/D_2-DR and **5**/D_2-DR were constructed from the coordinates of the potential energy minimum during the molecular dynamics simulation trajectory. Then, geometrical optimizations of the reduced model systems were carried out at semiempirical level employing a PM6 method with halogen bonding correction (PM6-D2X)[63] included in the MOPAC program.[64] The optimized models were then used as input for the calculation of the electron charge density topological analysis. Single point calculations were computed with Gaussian 03[65] employing a hybrid PBE functional and 6-31G(d) as basis set.

The topological properties of a scalar field such as $\rho(r)$ are summarized in terms of their critical points, i.e., the points r_c where $\Delta\rho(r) = 0$. Critical points are classified according to their type (ω,σ) by stating their rank, ω, and signature, σ. The rank is equal to the number of nonzero eigenvalues of the Hessian matrix of $\rho(r)$ at r_c, while the signature is the algebraic sum of the signs of the eigenvalues of this matrix. Critical points of $(3, -1)$ and $(3, +1)$ type describe saddle points, while the $(3, -3)$ is a maximum and $(3, +3)$ is a minimum in the field. Among these critical points, the $(3, -1)$ or bond critical points are the most relevant ones since they are found between any two atoms linked by a chemical bond. The determination of all the bond critical points and the corresponding bond paths connecting these point with bonded nuclei, were performed with the AIMAII software.[66]

3 Results and Discussion

As was pointed out in the introduction it is curious that until now it has not been reported the affinity for the D_2-DR of compound **3** which is relatively a simple molecule, at least from a structural point of view. One possible reason is that in that moment when the structurally related compounds were studied, this compound was discarded without an exhaustive analysis. It is also fair to note that at the time in which the analogues of compound **3** were reported it was not possible to perform theoretical calculations with a relatively detailed electronic analysis as has been done in this work. Anyway, the first thing we did was to synthesize compound 3 and then test its affinity for the D_2-DR.

3.1 Synthesis and Binding Affinity of 3-Chlorotyramine (Compound 3)

Compound **3** has been previously obtained by the Chung's method,[67] which consists in the oxidative chlorination of phenols with HCl and *m*-chloro perbenzoic acid (*m*-CPBA) in *N,N*-dimethyl formamide, and also using an enzymatic procedure.[68] In the course of our work on the synthesis of 1-substituted-1,2,3,4-tetrahydroisoquinolines,[22] the availability of the *N*-(4-(benzyloxy)-3-chlorophenethyl)benzamide (**1**) allowed us to obtain compound **3** by hydrolysis of the benzamide bond. Initially and unsuccessfully, various basic and acid conditions excessively strong for the hydrolysis of the benzamide (**1**) were assayed. Finally, we used a hydrolysis reaction in milder conditions,[69] a mixture of 2.5 N HCl/HOAc (4 : 1) at reflux for 42 h, which afforded the 3-chlorinated dopamine analogue (compound **3**) in good yield (Scheme 1).

In order to minimize the experimental errors due to the methodology employed we used a very similar experimental protocol to that reported in reference.[70] Our experimental measurements indicated that compounds **3** possess a *Ki* value of 0.146 μM. It should be noted that this compound displayed a significant affinity by the D_2-DR; In fact this compound displayed an affinity very similar to that reported for the endogen ligand DA (*Ki* = 0.52 μM).[70] This
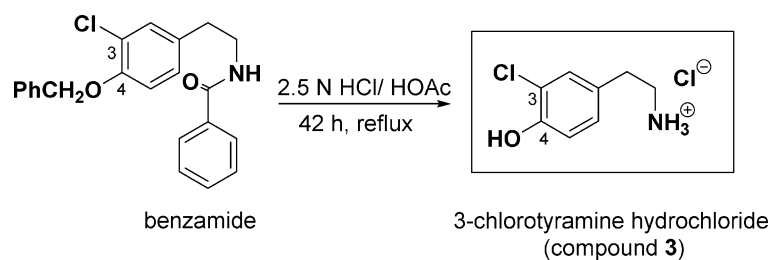
Scheme 1. Scheme of synthesis of compound **3**.

result was somewhat surprising to us since we expected a lower affinity for compound **3** relative to dopamine. After all the affinity reported for compound **2** is significantly lower than that of dopamine.[17] From these results we performed a molecular modeling study in which we analyzed exhaustively the molecular interactions in order to better understand these experimental results.

3.2 Molecular Dynamic Simulations

Comparing the MD trajectories obtained for the different complexes, interesting general conclusions might be obtained. Consistent with previous experimental[45–47] and theoretical[24,25] results, our simulations indicate the importance of the negatively charged aspartate 114 for the binding of these ligands. It is well-known that a highly conserved aspartic acid (D114) in transmembrane 3 (TM3) is important for the binding of both agonists and antagonists to the D_2-DR.[24,71,72] In the present study, all the compounds simulated were docked into the receptor with the protonated amino group near D114. After 10 ns of MD simulations, the ligands had moved slightly but in a different form compared with the initial position. However, the strong interaction with D114 was maintained for all the complexes (see figures 2–5) which support that D114 is the anchoring point for ligands with a protonated amino group.

In the next step of our study we evaluated the relative free energy ($\Delta(\Delta G_{bind})$) obtained for the different complexes (table 1, second column). The results obtained for compounds **4** and **5** were as expected since both compounds showed a lower affinity for the D_2-DR than compound **1**. Regarding compounds **2** and **3** and from the relative binding energies obtained in our MD simulations, one can appreciate that replacing the OH in *meta* (*m*-OH) by a chlorine atom increases the affinity for the D_2-DR in comparison to compound **1**, indicated by the lowest value of the relative free energy obtained for compound **3**. In contrast replacing the OH in *para* position (*p*-OH) displays the opposite effect, ie decreases the affinity for the receptor (5.57 kcal/mol above the value obtained for **3**). These results are at least qualitatively in agreement with the experimental results previously reported for compounds **1**, **2**, **4** and **5**[17,70,73] as well as with the experimental results reported here for compound **3**. To try to better understand these results we

compared the results obtained for **1**/D_2-DR complex with those complexes obtained for compounds **2–5**.

Figures 2 and 3 show the complexes obtained for compounds **3** and **2**, respectively, superimposed to complex **1**/D_2-DR for comparison. Figures 1S and 2S (electronic supporting material) show complexes **5**/D_2-DR and **4**/D_2-DR, respectively.

The superposition of the complexes **1**/D_2-DR and **3**/D_2-DR (see Figure 2) shows that both structures are very similar of the orientation of the ligand in the receptor binding site. In both complexes the ligand adopts extended conformation (torsional angle $\phi1=171°$ and $177°$ respectively; see Figure 1 for $\phi1$ definition) and the aromatic ring of compound **3** overlaps almost perfectly with the catecholic ring of **1**, with the difference that the first one is rotated $180°$ with respect to dopamine ring. In contrast, the superimposition of complexes **2**/D_2-DR and **1**/D_2-DR (see Figure 3) reveals a marked deviation of compound **2** orientation with respect to DA, with the first one displaying a smaller value of the $\phi1$ torsional angle ($\phi1=97°$).

Moreover, by comparison of chlorine atom binding mode in both chlorinated analogues one can see that in complex of compound **2** the chlorine atom is located in an hydrophobic environment composed of residues I184, F389, V190 and C—H bonds from H393 whereas in complex of compound **3** the same atom establishes interactions with the more polar residues S193 and S194.

3.3 Conformational Change in the Transmembrane 5 (TM5) Domain

Figures 4A and 4B give a different spatial view of the same complexes shown in Figures 2 and 3. One can see in these figures that in complexes **1**/D_2-DR and **3**/D_2-DR (see Figure 4A) the side-chain of S197 from transmembrane 5 (TM5) domain interacts with T119 from transmembrane 3 (TM3) domain. In contrast, in **2**/D_2-DR complex (see Figure 4B) this interaction has been disrupted during the MD simulation and the side chain of S197 associates with the backbone of residue S193 from the same TM5, causing distortion of the backbone interactions of TM5 and therefore the change in the structure of this transmembrane domain. It is worth noting that the change experienced by TM5 domain the complex **2**/D_2-DR reflects the importance of
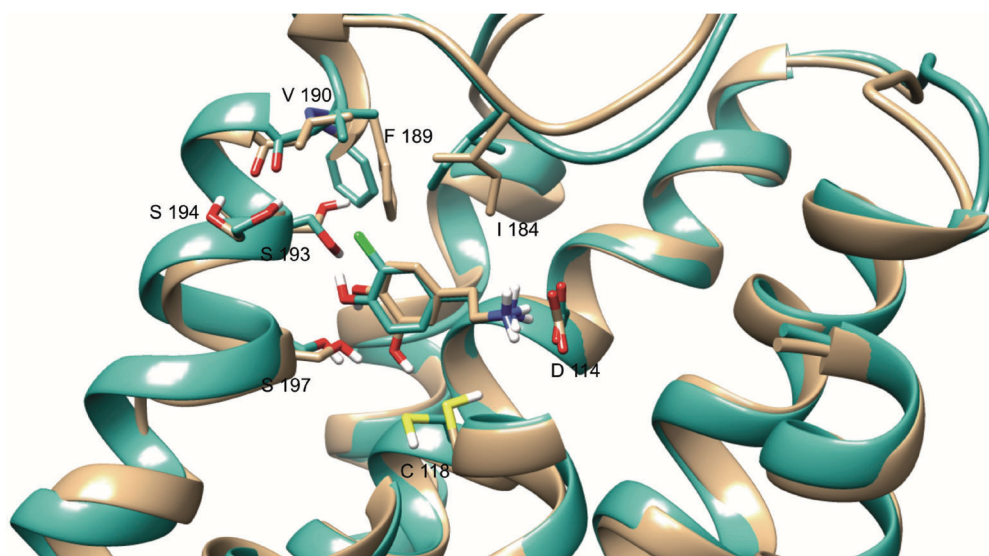
Figure 2. Spatial view of complex **3**/D$_2$-DR (cyan). Complex **1**/D$_2$-DR (in gray) is overimposed for comparison.
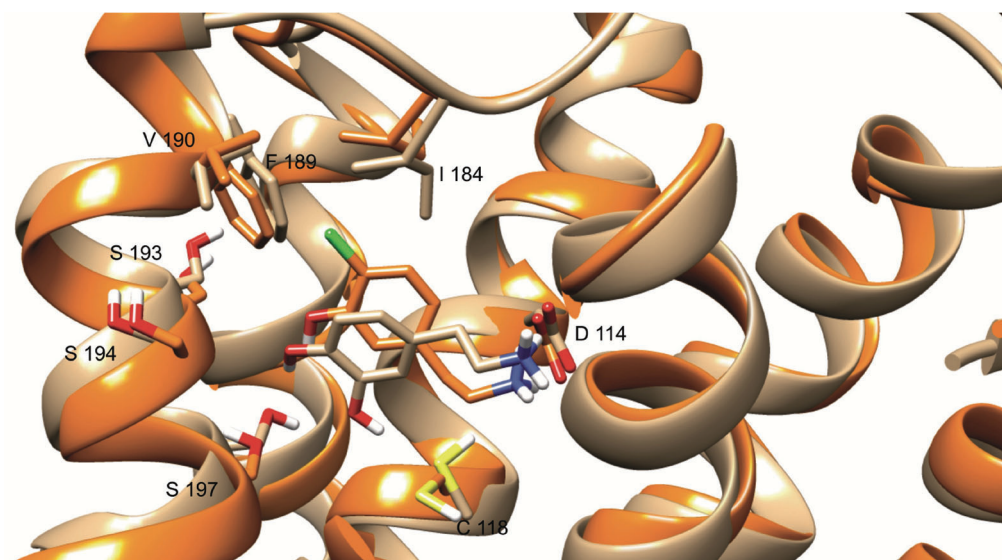

Figure 3. Spatial view of complex **2**/D$_2$-DR (orange). Complex **1**/D$_2$-DR (in gray) is overimposed for comparison.

preserving the flexibility of the backbone of TM5 during the simulation, as suggested by other authors.[53,74]

3.4 Possible Role of the Aromatic Residues of the Binding Site

From Figures 4A and 4B one also can see how the spatial distribution of the aromatic residues of the binding pocket of complexes **2**/D$_2$-DR and **3**/D$_2$-DR differs from that of complex **1**/D$_2$-DR. Figure 4A shows that the side chains of F389, F390 and F198 overlap almost perfectly in complexes **1**/D$_2$-DR and **3**/D$_2$-DR. These three residues are linked together by C$-$H·π interaction type (some of these interac-

tions are shown in the molecular graphs later) forming a conserved structure that has been observed also in D$_2$-DR complexes with alkaloids possessing a tetrahidroprotoberberine structure.[49] This conserved structure forms specific interactions with the ligand, contributing, together with the principal interaction D114 to its anchoring in the proper orientation within the binding site. On the other hand, in complex **2**/D$_2$-DR the side chains of the phenylalanine triad show a marked deviation in its rings spatial distribution relative to **1**/D$_2$-DR (see Figure 4B). This alteration in the phenylalanine triad structure is a consequence of the distortion that TM5 undergoes in the **2**/D$_2$-DR complex, which produces a displacement of the F198 (residue that
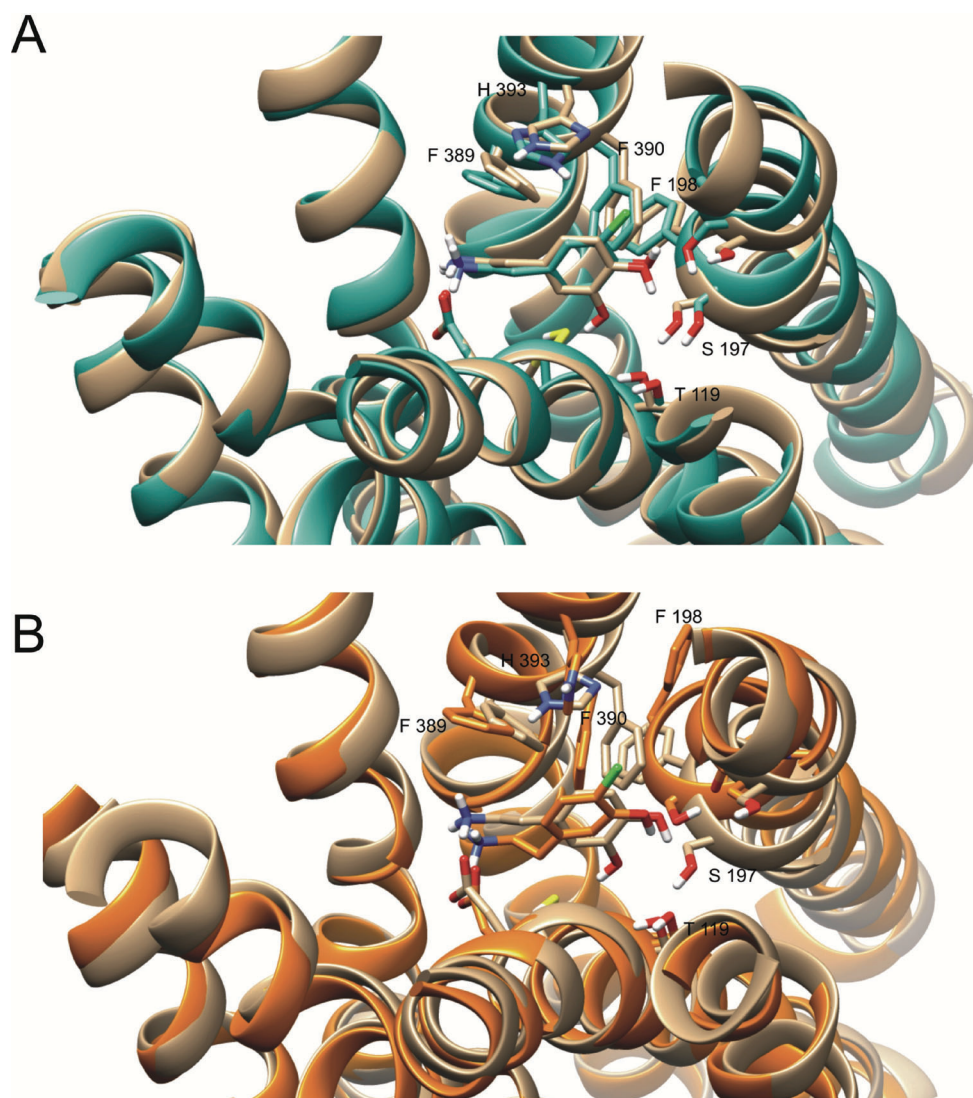
Figure 4. Similar spatial view to that shown in Figure 2 (4A) and 3 (4B) but in this case displaying the spatial distribution of the aromatic residues of the binding site.

belongs to TM5) so that it can no longer be associated with F190. Since phenylalanine triad produces specific interactions with the ligand, the alteration of its structure necessarily affects the binding mode of the ligand into the binding site, being this another factor that helps to explain the change in orientation of compound **2** within the binding site with respect to compounds **1** and **3**.

At this stage of our work we consider the trend predicted for the MD simulations as certainly significant but, on the other hand the approximations involved in this approach compels us to go beyond the classical treatment of the interactions to confirm our results. It should be noted that we are dealing with relatively weak interactions and therefore MD simulations might underestimate such interactions. Thus, in the next step of our study we constructed reduced model systems using combined semiempirical and DFT calculations.

3.5 Constructing the Reduced Models for the Binding Site

Figure 5 shows the ligand-residue interaction spectra calculated by the per residue free energy decomposition, which suggests that the interaction spectra of compounds **1**–**5** with D_2-DR are closely related and reflects their similar binding modes. As shown in Figure 5, the residues D114 and V115 are those with the greatest contribution to the interaction energy, this is true not only for compounds **1**–**5**, but also for other compounds with dopaminergic activity previously reported.[49]

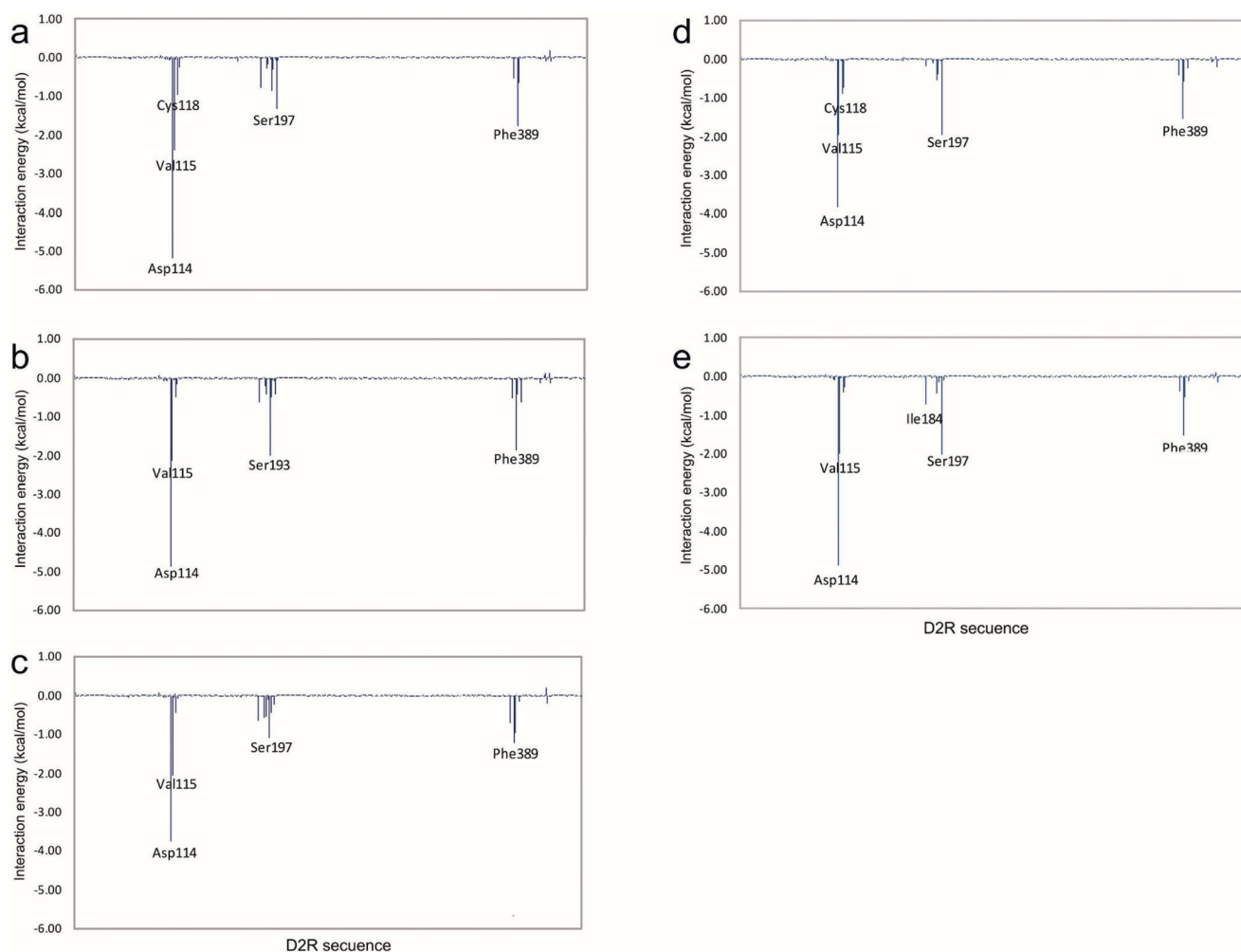Since the salt bridge with D114 is the strongest interaction established in the binding site it is considered a guide-

Figure 5. Histograms of interaction energies partitioned for D_2-DR amino acids when complexed with compound 1 (a), compound **3** (b), compound **2** (c), compound **5** (d) and compound **4** (e). The *x*-axis denotes the residue number of D_2-DR, and the y-axis shows the interaction energy between the compound and the specific residue. Negative and positive values represent favorable or unfavorable binding, respectively.

line interaction for ligand anchoring into the D_2-DR binding site. With respect to V115, this amino acid forms several C—H·π interactions with the aromatic ring of dopamine. These interactions are not shown in the molecular graphs displayed below for easy viewing of the molecular interactions of *meta*-OH/Cl and *para*-OH/Cl. Moreover, among the serine residues of the binding site, S197 is the residue that has the largest contribution to the interaction energy in complexes **1**/D_2-DR and **2**/D_2-DR, being higher in the first one, while S193 presents the most important contribution in the complex **3**/D_2-DR. Finally, the residue decomposition analysis also shows a significant contribution of one of the residues of the phenylalanine triad, F389, its contribution being greater in **1**/D_2-DR and **3**/D_2-DR than in **2**/D_2-DR.

From these results we considered prudent to include in the reduced model not just those amino acids involved in the most relevant molecular interactions displayed in the different spectra, but also all the residues involved in stabi-

lizing and destabilizing interactions showing non negligible contribution in the per residue energy decomposition spectra. Thus, residues D114, V115, M116, C118, T119, I184, F189, V190, V191, Y192, S193, S194, I195, V196, S197, F198, W386, F389, F390, H393, Y408, T412 and Y416 were included in the reduced model for the binding pocket of D_2-DR and therefore a final number of 23 amino acids were included in our model. A spatial view of this reduced model is shown in Figure 6.

3.6 Quantum Mechanics Calculations and Topological Analysis of the Electron Density

The starting geometries for each complex were obtained from the coordinates of the potential energy minimum during the simulation time. PM6-D2X optimizations were performed by considering the mentioned 23 residues from the receptor binding pocket. Next, DFT (PBE/6-31G(d)
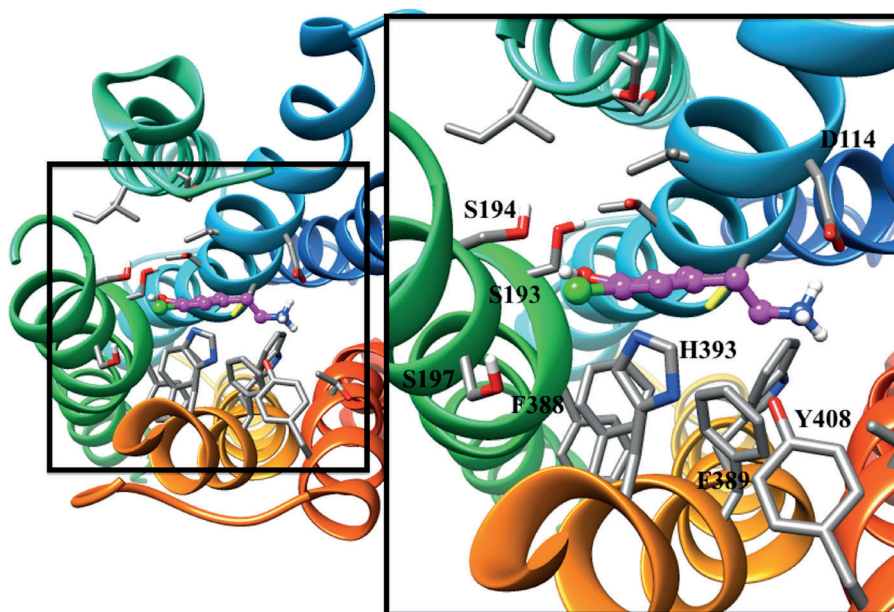
Figure 6. Spatial view of compound **3** (magenta)/D$_2$-DR interaction. Magnification of the receptor active site at the right. The names of the residues involved in the main interactions are written in the figure.

single point calculations were carried out for each of the PM6-D2X optimized complexes.

3.7 Evaluating the Molecular Interactions for the Different Complexes

On the basis of the results obtained from the MD simulations we focused the quantum mechanical analysis on dopamine (compound **1**) and its two chlorinated analogues (compounds **2** and **3**).

Figure 7 gives the values of ρ_b summation ($\Sigma\rho_b$) corresponding to all the intermolecular interactions (Figure 7A) and only those interactions involving substituent in the *meta* (*m*-OH/Cl) and *para* positions (*p*-OH/Cl) (Figure 7B) of compounds **1**–**3** at the D$_2$-DR binding site.

In accordance with the relative free energy data (see Table 1) the $\Sigma\rho_b$ values corresponding to all the intermolecular interactions (Figure 7A) shows that compounds **3** and **2** are more strongly and more weakly anchored to the D$_2$-DR binding site than compound **1**, respectively.

Table 1. Relative free energy ($\Delta(\Delta G_{bind})$) obtained in kcal/mol for the five complexes studied here. IC_{50} experimental values are given in the second column.

Complex	$\Delta(\Delta G_{bind})$	IC_{50} (µM)	Reference
1/D$_2$-DR	3.10	0.52	[41]
2/D$_2$-DR	5.57	26.31	[9]
3/D$_2$-DR	0.00	0.15	This work
4/D$_2$-DR	4.84	> 300	[42]
5/D$_2$-DR	4.00	26.5	[42]

Figures 8, 9 and 10 show the molecular graph of electron density obtained for compounds **1**, **3** and **2** in the D$_2$-DR binding site, respectively.

3.8 Catechol Interactions

The molecular graph of Figure 8 shows the most important interactions of compound **1** with the residues of the binding site. In particular, it is observed that OH in the *meta* position (*m*-OH) establishes a strong O—H·S hydrogen bond (HB) with C118 ($\rho_b = 0.0202$ au), other weaker HBs of the type C—H·O with F390 ($\rho_b = 0.0023$ au), S197 ($\rho_b = 0.0065$ au) and V115 ($\rho_b = 0.0032$ au) and two O·O contacts with T119 ($\rho_b = 0.0061$ au) and S197 ($\rho_b = 0.0072$ au). While in position *para* the OH behaves as a proton donor against S197 ($\rho_b = 0.0212$ au), and as proton acceptor against C—H bonds of F390 ($\rho_b = 0.0034$ au). Furthermore, like *m*-OH, *p*-OH also establishes a contact of the type O·O with backbone of S193 ($\rho_b = 0.0027$ au).

It is important to highlight the three O·O interactions in the **1**/D$_2$-DR complex. Even more interesting, the oxygen atoms of S197 and T119 that are engaged to the oxygen in *meta* position (*m*-O) are connected each other through a strong OH·O hydrogen bond. Thus, the three oxygen atoms are connected directly or indirectly by bond paths to give a topological ring (see Figure 7). This kind of O·O contacts has been already described in previous reports[25,49] and in such sense we believe they could be involved in the ligand/receptor recognition process.
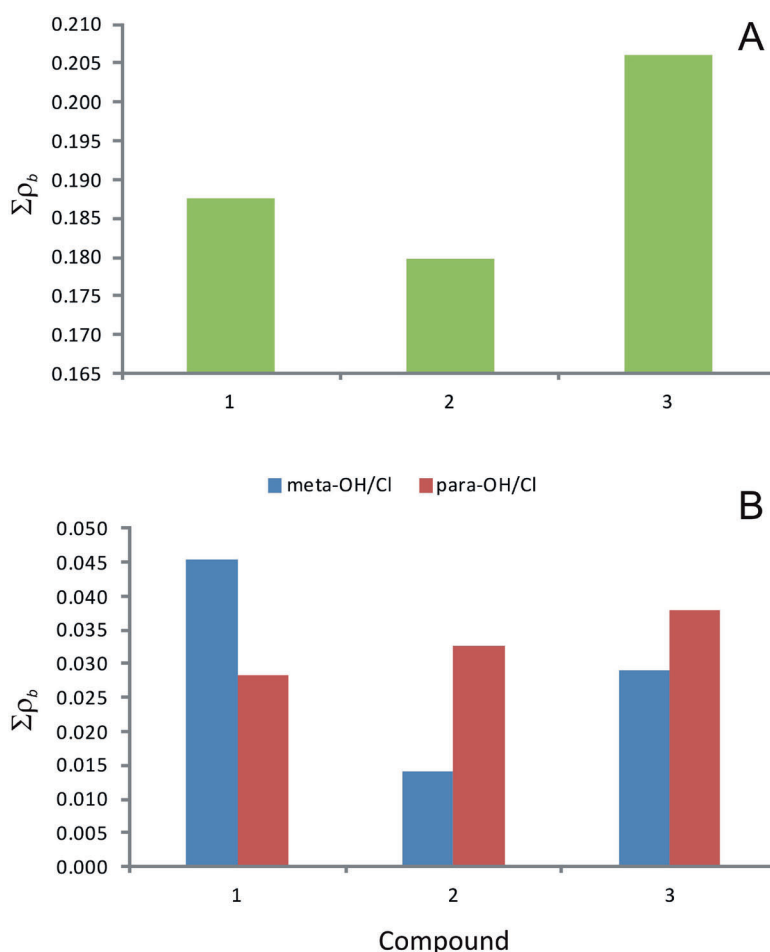
Figure 7. $\Sigma\rho_b$ values obtained for all the intermolecular interactions (7A) and only those involving substituents in meta (*m*-OH/Cl) and position (p-OH/Cl) (7B) of compounds **1–3** at the D$_2$-DR binding site.

3.9 Interactions of the Chlorine Atom

As can be seen in Figure 9, the chlorine atom of compound **3** (in *meta* position, *m*-Cl) establishes six interactions with the binding site of D$_2$-DR. Three C—H·Cl interactions with residues I184, V190 and H393 ($\Sigma\rho_b = 0.0149$ au), two interactions of the O·Cl type with S193 ($\rho_b = 0.0128$ au) and S194 ($\rho_b = 0.0013$ au) and a strong intramolecular (O—)H·Cl HB interaction with the OH in *para* position ($\rho_b = 0.0240$ au).

Moreover, in complex of compound **2**, the chlorine atom is more "buried" in the hydrophobic region (see Figure 10) forming only C—H·Cl interactions (a total of six interactions with residues I184, F189, V190 and H393 ($\Sigma\rho_b = 0.0326$ au)). Note that in this complex the chlorine atom is not forming an intramolecular HB with *m*-OH as in the case of compound **3**.

The two Cl·O interactions that are only established in complex **3**/D$_2$-DR could explain the favorable binding behavior observed for compound **3**. In other words, the Cl·O in complex **3**/D$_2$-DR might be mimicking the behavior of

the dopamine O·O interactions with carbonyl and hydroxyl groups of the biological receptor.

Going back to Figure 7B, the ρ_b summation ($\Sigma\rho_b$) corresponding to interactions of *m*-Cl and *p*-Cl shows that the chlorine atom in compound **2** is more strongly anchored to the D$_2$-DR binding pocket than the same atom in compound **3**. Thus, based in these results, it is fair to say that the chlorine atom prefers to be in an hydrophobic environment as in complex **2**/D$_2$-DR where only C—H·Cl interactions are formed rather than a more polar one, as in complex **3**/D$_2$-DR where two Cl·O interactions are established.

On the basis of this results, the next question one might ask is what then makes compound **3** be more strongly anchored to the D$_2$-DR binding site than compound **2**? This issue is explored in the next section.

3.10 Effects of the Chlorine Substitutions on the Interactions of the OH Groups

Figure 7B shows that when the OH in *meta* position of compound **1** is replaced by a chlorine atom as in com-
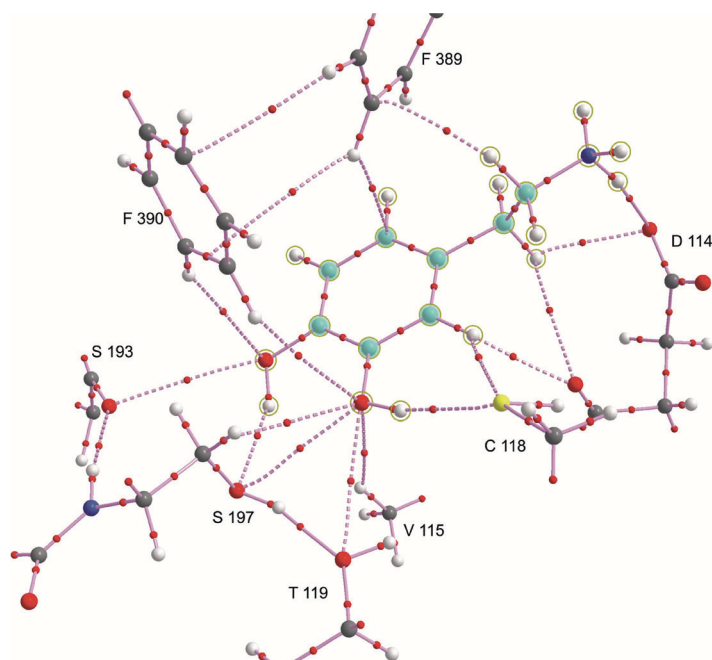
Figure 8. Molecular graph of compound **1** at the D$_2$-DR binding site. Large spheres represent attractors or nuclear critical points (3, −3) attributed to the atomic nuclei. Lines connecting the nuclei are bond paths and small spheres on them are bond critical points (3, −1).
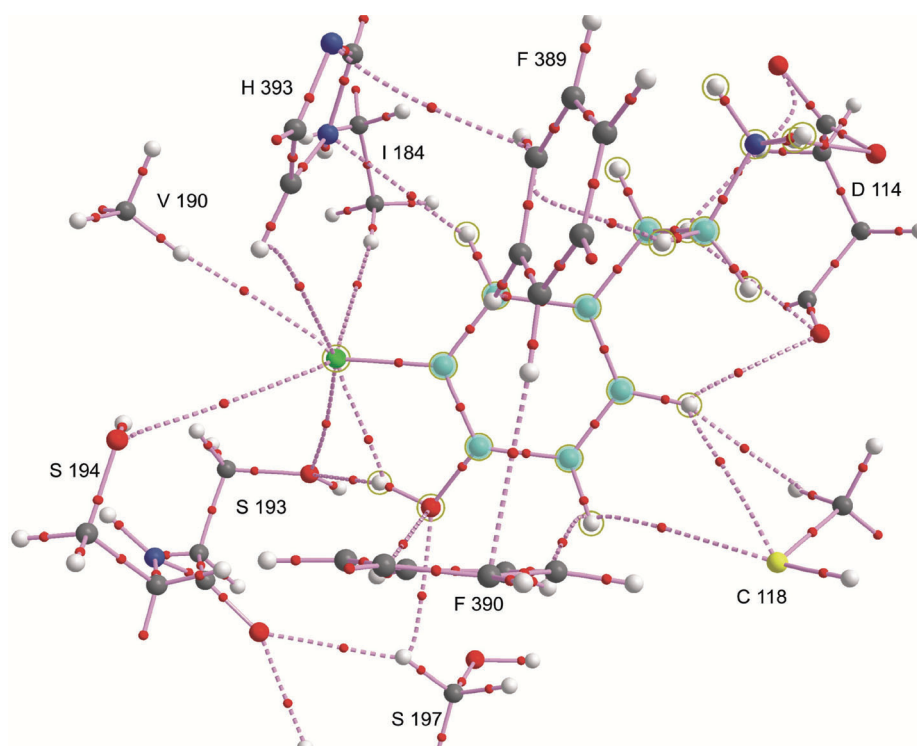

Figure 9. Molecular graph of compound **3** at the D$_2$-DR binding site. Large spheres represent attractors or nuclear critical points (3, −3) attributed to the atomic nuclei. Lines connecting the nuclei are bond paths and small spheres on them are bond critical points (3, −1).

pound **3**, it cannot be anchored to the binding site with the same force as the *m*-OH of compound **1**. However, the introduction of Cl at *meta* position improves the interac-

tions of p-OH with respect to the same group in **1**. Thus, both groups together, *m*-Cl and *p*-OH are anchored to the binding site with almost the same strength as the corre-
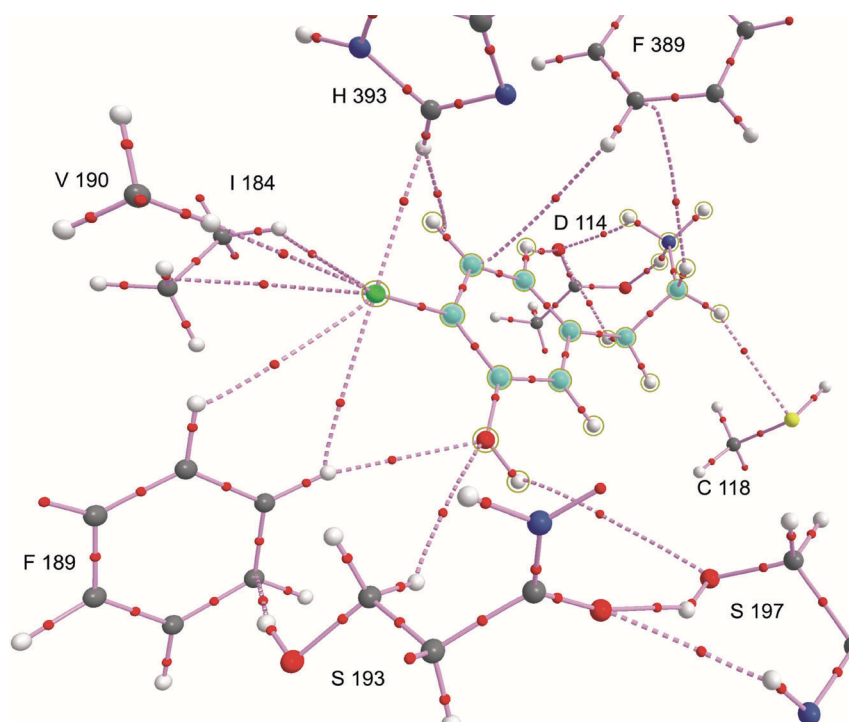
Figure 10. Molecular graph of compound **2** at the D$_2$-DR binding site. Large spheres represent attractors or nuclear critical points (3, −3) attributed to the atomic nuclei. Lines connecting the nuclei are bond paths and small spheres on them are bond critical points (3, −1).

sponding catecholic hydroxyls of **1**. Thus, the presence of the chlorine atom in the *meta* position modifies the binding site (throught the Cl·O interactions with serine residues) in order to strengthen interaction of *p*-OH.

On the other hand, when *p*-OH of compound **1** is replaced by chlorine as in compound **2**, the halogen provides stronger interactions than the corresponding OH group. However, the introduction of chlorine significantly weakens the interactions of *m*-OH in comparison to the same group in **1**/D$_2$-DR complex, so that both groups together bind much more weakly to the binding site that the corresponding OH groups of compound **1**.

As discussed above, in complex **2**/D$_2$-DR the chlorine atom is more "buried" in the hydrophobic pocket formed by residues I48, F154 and V190 that in the **3**/D$_2$-DR complex. This determines that *m*-OH be poorly positioned to interact with the serines of the binding site.

Summarizing the results of the molecular modeling section, it was shown that the binding mode of compound **3** in the D$_2$-DR binding pocket resemble the DA binding mode (see Figure 2) whereas in compound **2**, the anchoring of the chorine atom in an hydrophobic pocket determines a different binding mode for this compound (see Figure 3). While the chlorine atom in compound **2** is more strongly anchored in the D$_2$-DR binding pocket than the same atom in compound **3** (Figure 7B), the overall binding of the last compound is stronger than the first one (Table 1 and Figure 7A) in part due to the better placement of the

hydroxyl group to interact with the serine residues from the receptor binding pocket. Furthermore, it was shown that the binding mode of compound **2** to D$_2$-DR determines a distortion of TM5 that in turn disturbs specific interactions between phenylalanine resides of the binding pocket and the ligand (Figures 4A,B).

3.11 Scope and Limitations of the Methodology Used Here

Let us now make some comments on the scope and limitations that might have the application of calculations used in this work.

With respect to the applicability to other biological systems, It is important to note that studies using molecular techniques QTAIM applied to large systems of biological interest are relatively new and therefore there are few studies previously reported in the literature. However, it is important to note that these simulations have been used successfully in inhibitors of dihydrofolate reductase (DHFR)[48] as well as with BACE 1 inhibitors.[75,76] Although the types of receptors studied so far are very few, at least it is interesting to note that it is possible to do this kind of simulations successfully in different types of receptors. Now we are doing studies on different types of ligand-receptor complexes with different types of interactions (from very strong to very weak ones). It is clear that the results obtained in such study will give us a better picture about the scope of applicability of the simulations used here.

With respect to the applicability of these simulations to structurally unrelated chemotypes. We have recently reported some works in which we have studied compounds structurally different with this type of approach.[25,49,50] In a study of DHFR inhibitors it was possible to include in the correlation two new series of compounds possessing significant structural differences with respect to the known classical and non-classical inhibitors.[48] In the particular case of D_2-DR in previous works we have reported the analysis of BTHIQs compounds[24] as well as of protoberberine derivatives[49] by using this type of simulations. While the structural variability is still very meager, the results obtained so far are very promising for this kind of approach using reduced models and QTAIM calculations. Thus, it appears very reasonable that these simulations might be successfully applied to compounds with different structural chemotypes. Importantly, in all the above cases, these studies including quantum mechanical calculations and QTAIM studies have significantly improved correlations between experimental and theoretical results in a quantitative mode which indicates how valuable is this protocol for prioritizing certain chemotypes.

A somewhat negative aspect also needs to be highlighted. The protocol used is far from to be considered a post-docking routine method in its current form. However, considering that the type of calculations performed are not particularly sophisticated, it would be possible to design a protocol developing the various steps in a more systematic and friendly way. We are working on it.

4 Conclusions

In this paper we performed a molecular modeling study of 3-chlorotyramine and analogues. The theoretical and experimental results reported here allowed us to reach at least two interesting conclusions. On one side we are reporting that 3-chlorotyramine has a D_2 receptor affinity that it is comparable to that of the endogenous ligand (dopamine). This result is very interesting because until now it has been reported that all halogenated dopamine derivatives have a significantly lower affinity for both D_1 and D_2 receptors. On the other hand it should be noted that our theoretical study (including a comprehensive analysis of the molecular interactions) has been able to explain such a significant affinity of 3-chlorotyramine for the D_2 receptor. However, it is important to note that in order to evaluate in detail the various molecular interactions of ligands at its site of action, it is necessary to use reduced models systems which allow to perform quantum mechanical calculations and QTAIM type studies. While these calculations require more time than traditional or standard simulations, apparently this effort is justified because it allows a deeper and more appropriate description of the ligand-receptor interactions.

By combining MD simulations with semiempirical and DFT calculations, a simple and generally applicable procedure to evaluate the binding energies of ligands interacting with the D_2-DR has been reported here. Thus, our theoretical and experimental results contribute to the understanding of the non covalent interactions in the context of the ligand - receptor binding event in a two-way manner, by providing a detailed topological description of the interaction network of the ligand in the receptor binding pocket and by showing the convenience of going beyond the concept of pair-wise interactions in order to "see" the electronic effects within the intricate biological environment. Undoubtedly the results presented here show the importance of performing these studies as comprehensive as possible when hydrogen bonds are involved and even more if there are halogen atoms involved in these interactions. Thus, we believe our results may be helpful in the structural identification and understanding of the minimum structural requirements for these molecules and can provide a guide in the design of new ligands for the D_2 receptor of dopamine.

List of the Abbreviations

QTAIM	Quantum theory of atoms in molecules
DR	Dopamine receptor
DA	Dopamine
MD	Molecular dynamics
BTHIQs	Benzyl-tetrahydroisoquinolines

Acknowledgements

References

[1] L. Bettinetti, S. Löber, S. Hübner, P. Gmeiner, *J. Comb. Chem.* **2005**, *7*, 309–316.

[2] J. W. Kebabian, F. I. Tarazi, N. S. Kula, R. J. Baldessarini, *Drug Discov. Today* **1997**, *2*, 333–340.

[3] R. J. Baldessarini, in *The Dopamine Receptors* (Eds: K. A. Neve, R. L. Neve), Humana Press, Totowa, NJ, **1997**, 457–498.

[4] R. B. Mailman, D. E. Nichols, A. Tropsha, in *The Dopamine Receptors* (Eds: K. A. Neve, R. L. Neve), Humana Press, Totowa, NJ, **1997**, 105–133.

[5] J. P. Kelleher, F. Centorrino, M. J. Albert, R. J. Baldessarini, *CNS Drugs.* **2002**, *16*, 249–261.

[6] M. Rowley, L. J. Bristow, P. H. Hutson, *J. Med. Chem.* **2001**, *44*, 477–501.

[7] M. Reutlinger, T. Rodrigues, P. Schneider, G. Schneider, *Angew. Chem. Int. Ed.* **2014**, *53*, 1–6.

[8] a) J. A. Hiss, M. Hartenfeller, G. Schneider, *Curr. Pharm. Des.* **2010**, *16*, 1656–1665; b) J. A. Hiss, M. Reutlinger, C. P. Koch, A. M. Perna, P. Schneider, T. Rodrigues, S. Haller, G. Folkers, L. Weber, R. B. Baleeiro, P. Walden, P. Wrede, G. Schneider, *Future Med. Chem.* **2014**, *6*, 267–280.

[9] G. Gallagher, P. J. Lavanchy, J. W. Wilson, J. P. Hieble, R. M. Marinis, *J. Med. Chem.* **1985**, *28*, 1533–1536.

[10] K. L. Kirk, C. R. Creveling, *Med. Res. Reu.* **1984**, *4*, 189–220.

[11] R. M. De Marinis, G. Gallagher, R. F. Hall, R. G. Franz, C. Webster, W. F. Huffmann, M. S. Schwartz, C. Kaiser, S. T. Ross, J. W. Wilson, P. Hieble, *J. Med. Chem.* **1986**, *29*, 939–947.

[12] J. R. McCarthy, J. McCowan, M. B. Zimmerman, M. A. Wenger, L. W. Emmert, *J. Med. Chem.* **1986**, *29*, 1586–1590.

[13] J. Weinstock, D. E. Gaitanopouloe, O. D. Stringer, R. G. Franz, J. P. Hieble, L. B. Kinter, W. A. Maan, K. E. Flaim, G. Gessner, *J. Med. Chem.* **1987**, *30*, 1166–1176.

[14] L. Nedelec, C. Dumont, C. Obrlander, D. Frechet, J. Laurent, J. R. Bohier, *Eur. J. Med. Chem.* **1978**, *13*, 553–563.

[15] M. Cardellini, G. M. Cingolani, F. Claudi, V. Perlini, W. Balduini, F. Cattabeni, *Farmaco Ed. Sci.* **1988**, *43*, 49–59.

[16] F. Claudi, M. Cardelhi, G. M. Ciolani, A. Piergentili, G. Peruzzi, W. Balduini, SynWi, *J. Med. Chem.* **1990**, *33*, 2408–2412.

[17] F. Claudi, G. Giorgioni, A. Di Stefano, M. P. Abbracchio, A. M. Paoletti, W. Balduinio, *J. Med. Chem.* **1992**, *35*, 4408–4414.

[18] J. Weinstock, D. E. Gaitanopoulos, O. Hye-Ja, F. R. Pfeiffer, C. B. Karaeh, J. W. Venslavsky, H. M. Sarau, K. E. Flaim, J. P. Hieble, C. Kaiser, *J. Med. Chem.* **1986**, *29*, 1613–1627.

[19] R. W. Fuller, J. Mills, M. M. Marsh, *J. Med. Chem.* **1971**, *14*, 322–325.

[20] P. Stark, W. Fuller, *Neurophormacology* **1972**, *11*, 261–272.

[21] K. M. O'Boyle, J. L. Waddington, *Eur. J. Pharmacol.* **1985**, *115*, 291–295.

[22] I. Berenguer, N. El Aouad, S. Andujar, V. Romero, F. Suvire, T. Freret, A. Bermejo, M. D. Ivorra, R. D. Enriz, M. Boulouard, N. Cabedo, D. Cortes, *Bioorg. Med. Chem.* **2009**, *17*, 4968–4980.

[23] N. El Aouad, I. Berenguer, V. Romero, P. Marín, A. Serrano, S. Andujar, F. Suvire, A. Bermejo, M. D. Ivorra, R. D. Enriz, N. Cabedo, D. Cortes, *Eur. J. Med. Chem*, **2009**, *44*, 4616–4621.

[24] S. Andujar, F. Suvire, I. Berenguer, N. Cabedo, P. Marín, L. Moreno, M. D. Ivorra, D. Cortes, R. D. Enriz, *J. Mol. Model.* **2012**, *18*, 419–431.

[25] S. A. Andujar, R. D. Tosso, F. D. Suvire, E. Angelina, N. Peruchena, N. Cabedo, D. Cortes, R. D. Enriz, *J. Chem. Inf. Model.* **2012**, *52(1)*, 99–112.

[26] U. Koch, P. L. Popelier, *J. Phys. Chem.* **1995**, *99*, 9747–9754.

[27] C. F. Matta, N. Castillo, R. J. Boyd, *J. Phys. Chem. B* **2005**, *110*, 563–578.

[28] R. A. Mosquera, M. J. G. Moa, L. Estévez, M. Mandado, A. M. Graña, in *Quantum Biochemistry* (Ed: C. F. Matta), Wiley-VCH, Weinheim, Germany, **2010**.

[29] J. M. Dumas, H. Peurichard, M. Gomel, *J. Chem. Res.* **1978**, *2*, 54–55.

[30] T. Clark, M. Hennemann, J. S. Murray, P. Politzer, *J. Mol. Model.* **2007**, *13(2)*, 291–296.

[31] T. Clark, *σ-Holes*, *Comput. Mol. Sci.* **2012**, DOI: 10.1002/wcms.1113.

[32] A. Legon, *Phys. Chem. Chem. Phys.* **2010**, *12*, 7736–7747.

[33] A. C. Legon, *Angew. Chem., Int. Ed.* **1999**, *38*, 2686–2714.

[34] P. Politzer, J. S. Murray, T. Clark, *Phys. Chem. Chem. Phys.* **2010**, *12*, 7748–7757.

[35] C. Bissantz, B. Kuhn, M. Stahl, *J. Med. Chem.* **2010**, *53(14)*, 5061–5084.

[36] L. A. Hardegger, B. Kuhn, B. Spinnler, L. Anselm, R. Ecabert, M. Stihle, B. Gsell, R. Thoma, J. Diez, J. Benz, J. M. Plancher, G.

Hartmann, D. W. Banner, W. Haap, F. Diederich, *Angew. Chem., Int. Ed.* **2011**, *50(1)*, 314–318.

[37] L. A. Hardegger, B. Kuhn, B. Spinnler, L. Anselm, R. Ecabert, M. Stihle, B. Gsell, R. Thoma, J. Diez, J. Benz, J. M. Plancher, G. Hartmann, Y. Isshiki, K. Morikami, N. Shimma, W. Haap, D. W. Banner, F. Diederich, *ChemMedChem.* **2011**, *6(11)*, 2048–2054.

[38] R. Wilcken, X. Liu, M. O. Zimmermann, T. J. Rutherford, A. R. Fersht, A. C. Joerger, F. M. Boeckler, *J. Am. Chem. Soc.* **2012**, *134(15)*, 6810–6818.

[39] H. G. Kümmel, *Biography of the Coupled Cluster Method*; World Scientific, Singapore. **2002**.

[40] C. Møller, M. S. Plesset, *Phys. Rev.* **1934**, *46(7)*, 618.

[41] J. A. Pople, J. S. Binkley, R. Seeger, *Int. J. Quantum Chem.* **1976**, 1–19.

[42] Y. Lu, Y. Wang, W. Zhu, *Phys. Chem. Chem. Phys.* **2010**, *12(18)*, 4543–4551.

[43] Y. Lu, T. Shi, Y. Wang, H. Yang, X. Yan, X. Luo, H. Jiang, W. Zhu, *J. Med. Chem.* **2009**, *52(9)*, 2854–2862.

[44] P. Dobes, J. Rezáč, J. Fanfrlík, M. Otyepka, P. Hobza, *J. Phys. Chem. B* **2011**, *115(26)*, 8581–8589.

[45] C. Coley, R. Woodward, A. M. Johansson, P. G. Strange, L. H. Naylor, *J. Neurochem.* **2000**, *74(1)*, 358–366.

[46] R. Woodward, C. Coley, S. Daniell, L. H. Naylor, P. G. Strange, *J. Neurochem.* **1996**, *66(1)*, 394–402.

[47] B. A. Cox, R. A. Henningsen, A. Spanoyannis, R. L. Neve, K. A. Neve, *J. Neurochem.* **1992**, *59*, 627–635.

[48] R. D. Tosso, S. A. Andujar, L. Gutierrez, E. Angelina, R. Rodríguez, M. Nogueras, H. Baldoni, F. D. Suvire, J. Cobo, R. D. Enriz, *J. Chem. Inf. Model.* **2013**, *53*(8), 2018–2032.

[49] J. Párraga, N. Cabedo, S. Andujar, L. Piqueras, L. Moreno, A. Galán, E. Angelina, R. D. Enriz, M. D. Ivorra, M. J. Sanz, D. Cortes, *Eur. J. Med. Chem.* **2013**, *68*, 150–166.

[50] E. Angelina, S. A. Andujar, R. D. Tosso, R. D. Enriz, N. Peruchena, *Non-covalent interactions in receptor-ligand complexes. A study based on the electron charge density*. CLAFCO Congress, Foz Iguazu (Brasil), **2013**.

[51] R. Bader, *Atoms in Molecules: A Quantum Theory*, Oxford University Press, New York, **1990**.

[52] S. J. Grabowski, *J. Phys. Chem. A* **2012**, *116*, 1838–1846.

[53] M. A. Soriano-Ursúa, J. O. Ocampo-López, K. Ocampo-Mendoza, J. G. Trujillo-Ferrara, J. Correa-Basurto, *Comput. Biol. Med.* **2011**, *41*, 537–445.

[54] M. Y. Kalani, N. Vaidehi, S. E. Hall, R. J. Trabanino, P. L. Freddolino, M. A. Kalani, W. B. Floriano, V. W. Kam, W. A. Goddard 3rd, *Proc. Natl. Acad. Sci.* **2004**, *101*, 3815–3820.

[55] G. M. Morris, D. S. Goodsell, R. S. Halliday, R. Huey, E. Hart, R. K. Belew, A. J. Olson, *J. Comp. Chem.* **1998**, *19*, 1639–1662.

[56] W. L. Jorgensen, J. Chandrasekhar, J. D. Madura, R. W. Impey, M. L. Klein, *J. Chem. Phys.* **1983**, *79*, 926–935.

[57] D. A. Case, T. E. Cheatham, T. Darden, H. Gohlke, R. Luo, K. M. Merz Jr., A. Onufriev, C. Simmerling, B. Wang, R. J. Woods, *J. Comput. Chem.* **2005**, *26*, 1668–1688.

[58] D. A. Case, T. A. Darden, T. E. Cheatham III, C. L. Simmerling, J. Wang, R. A. Duke, R. Luo, R. C. Walker, W. Zhang, K. M. Merz, *AMBER12*, University of California, San Francisco. **2012**.

[59] T. Darden, D. York, L. Pedersen, *J. Chem. Phys.* **1993**, *98*, 10089–10092.

[60] U. Essmann, L. Perera, M. L. Berkowitz, T. Darden, H. Lee, L. G. Pedersen, *J. Chem. Phys.* **1995**, *103*, 8577–8593.

[61] T. Hou, N. Li, Y. Li, W. Wang, *J. Proteome Res.* **2012**, *11*, 2982–95.

[62] H. Gohlke, C. Kiel, D. A. Case, *J. Mol. Biol.* **2003**, *330*, 891–913.

[63] J. Řezáč, P. Hobza, *Chem. Phys. Lett.* **2011**, *506*, 286–289.

[64] J. J. P. Stewart, MOPAC2009 Stewart Computational Chemistry, Colorado Springs, CO, USA, **2008**.

[65] M. J. Frisch, G. W. Trucks, H. B. Schlegel, G. E. Scuseria, M. A. Robb, J. R. Cheeseman, J. A. Montgomery Jr., T. Vreven, K. N. Kudin, J. C. Burant, *Gaussian 03, Revision C05,*Gaussian, Inc., Wallingford, CT, **2004**.

[66] T. Keith, *AIMA11, 12.11.09*, Gristmill Software, Overland Park, KS, USA, **2012**.

[67] K. H. Chung, H. J. Kim, H. R. Kim, E. K. Ryu, *Synth. Commun.* **1990**, *20*, 2991–2997.

[68] H. Nakazawa, K. Sano, K. Matsuda, K. Mitsugi, *Biosci. Biotech. Biochem.* **1993**, *57*, 1210–1211.

[69] M. Alías, M. P. López, C. Cativiela, *Tetrahedron* **2004**, *60*, 885–891.

[70] L. B. Kozell, K. A. Neve, *Mol. Pharmacol.* **1997**, *52(6)*, 1137–1149.

[71] M. M. Teeter, M. F. Froimowitz, B. Stec, C. J. Durand, *J. Med. Chem.* **1994**, *37*, 2874–2888.

[72] A. Mansour, F. Meng, J. H. Meador-Woodruff, L. P. Taylor, O. Civelli, H. Akil, *Eur J Pharmacol.* **1992**, *227*, 205–214.

[73] S. L. Payne, A. M. Johansson, P. G. Strange, *J. Neurochem.* **2002**, *82(5)*, 1106–1117.

[74] V. Katritch, K. A. Reynolds, V. Cherezov, M. A. Hanson, C. B. Roth, M. Yeager, R. Abagyan, *J. Mol. Recognit.* **2009**, *22*, 307–318.

[75] L. J. Gutierrez, E. Angelina, N. Peruchena, H. A. Baldóni, R. D. Enriz, *Small-size peptides acting as inhibitors of the BACE1-exosite. A molecular modeling study using MD simulations and QM calculations*, 10th Congress of the World Association of Theoretical and Computational Chemists (WATOC), Santiago, Chile, **2014**. http://watoc2014.com/

[76] L. J. Gutierrez, *Search and molecular modeling study of the exosite of BACE1*, PhD Thesis, National University of San Luis (Argentina), **2013**.